Rapid microwave synthesis of magnetocaloric Ni–Mn–Sn Heusler compounds

Rapid Microwave synthesis of magnetocaloric Ni-Mn-Sn Heusler compounds

L. Trombi[a], F. Cugini[b,c], R. Rosa[d], N. Sarzi Amadè[b,c], S. Chicco[b], M. Solzi[b,c], P. Veronesi[a]

[a] *Department of Engineering "Enzo Ferrari", University of Modena and Reggio Emilia, Via VIvarelli 10, 41125 Modena, Italy.*

[b] *Department of Mathematical, Physical and Computer Sciences, University of Parma, Parco Area delle Scienze 7/A 43124 Parma, Italy.*

[c] *IMEM-CNR Institute, Parco Area delle Scienze 37/A 43124 Parma, Italia.*

[d] *Department of Sciences and Methods for Engineering, University of Modena and Reggio Emilia, via Amendola 2, 42122 Reggio Emilia, Italy.*

Abstract

The magnetocaloric $Ni_{50}Mn_{25}Sn_{25}$ Heusler compound was prepared via ultra-fast and sustainable microwave synthesis, by using the two ways hybrid microwave heating method. The structural, microstructural, magnetic and magnetocaloric properties of the prepared specimen are presented. The functional features of the synthetized sample result comparable with compounds obtained with other high-temperature preparation techniques that require larger amount of energy. The proposed time and energy-efficient preparation method could promote the development of large mass production routes of multifunctional huge-potential Heusler compounds, exploitable as active materials in thermomagnetic energy conversion machines and in other technological applications.

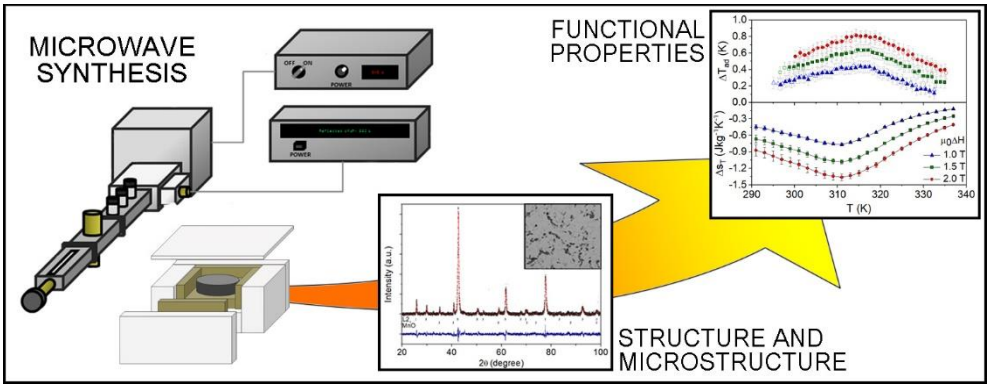

Key words

Heusler alloys, microwave synthesis, magnetocaloric effect, thermomagnetic energy conversion, magnetic cooling

Text

The Heuslers are a wide class of intermetallic compounds showing several multifunctional properties that make them promising materials for different technological applications [1]. Their extremely flexible structure allows the synthesis of compounds with different compositions presenting demanded functionalities. Their structural, electronic and magnetic properties can be tuned, allowing the exploitation, for example, of shape memory, thermoelectric and multi-caloric effects [1]. Heusler compounds are mainly studied for applications as mechanical actuators, sensors and as active materials in energy conversion devices, but the huge potential of this class of materials has not yet fully explored.

During the last decades, a great attention was paid on (Ni,Mn)-based magnetic Heusler compounds, as promising materials for magnetic energy conversion machines, as magnetic refrigerators and devices for the harvesting of otherwise wasted thermal energy [2,3]. $Ni_{50}Mn_{25+x}Z_{25-x}$ (with Z = Ga, In, Sn, Sb) Heusler compounds show, for a wide range of compositions, a large and tuneable magnetocaloric effect (MCE) both at the Curie transition of the ferromagnetic cubic phase (austenite) and at the first-order martensitic transition [4–8]. The possibility to easily tune their properties, the absence of rare earths and toxic elements and the high thermal conductivity make this class of materials very interesting for the above mentioned applications [3,9]. However, the high sensitivity of magnetic and magnetocaloric properties of these compounds to the composition, microstructure and to the degree of atomic order, increases the difficulties in preparing homogeneous materials with controlled and reproducible properties [10–14]. Thus, the development of procedures for the scale-up of laboratory preparation protocols is a challenging task. Conventionally, Heusler compounds are prepared by arc-melting [15], induction melting [16] or melt-spinning [17,18]. The use of high purity elements and a protective atmosphere are not sufficient to ensure a precise control of chemical composition: indeed, uncontrollable element-dependent weight losses usually occur [1]. Likewise, procedures of re-melting of the sample do not guarantee the required degree of homogeneity. One of the main causes is the development of high thermal gradients in the sample during the melting and the subsequent cooling. Long annealing treatments, from days to weeks, at high temperatures (T > 800K) under protective atmosphere are usually employed in order to improve the homogeneity of the as-cast samples [5,8].

In this work we introduce the use of Microwave (MW) Assisted Solid State Synthesis method for Mn-based magnetic Heusler compounds. Previously, only domestic microwave ovens were used for the preparation of different types of Half-Heuslers, thus without the possibility of a fine control and monitoring of the process parameters [19–21]. Microwave heating is part of the electro-heat techniques for heating of materials [22]. The specific feature of this technique is that the heat is generated inside the sample as a consequence of material-microwaves interaction, as opposed to other methods based on the transmission of heat from the surface to the centre of the sample (e.g. classic resistive ovens or arc-furnace) [23]. The synthesis takes place in extremely short time compared to other methods, and the obtained material usually possesses very homogeneous properties and does not require further homogenization heat treatment, with a typical gain in terms of time and energy consumption. Moreover, an extremely high degree of versatility can be obtained for MW heating based techniques, by varying several input parameters, among which dielectric and magnetic properties, heating mechanism, load arrangement/composition and the geometry of the employed microwave cavity have been recently recognized as the more significant ones [24]. By acting on the above mentioned parameters it is possible to finely tune the heating rate, to generate volumetric or local heating and to design demanded temperature profiles (positive, negative or neutral from the surface to the centre of the material) [25]. Moreover, even if scaling-up possibilities need to be considered

on a case to case basis, the above-mentioned versatility typically allows, also with the fundamental help of numerical simulation [26], together with the possibility to use less conventional microwave frequencies (with respect to the most widely employed 2450 MHz one) as well as opportunely designed cavities, to easily overcome limitations and issues arising from performing larger scale experiments [27].

$Ni_{50}Mn_{25}Sn_{25}$ Heusler compound was selected as test material for this work. This composition, free of critical and expensive elements, shows a Curie temperature of the austenitic phase just above room temperature and a saturation magnetization slightly lower than that of the corresponding In-based compound.
The synthesis of the compound was performed starting from elemental powders of Ni (-325 mesh, 99.8% purity), Mn (-325 mesh, 99.5% purity) and Sn (<45 μm, 99.8% purity), all of which were purchased from Alfa Aesar (Karlsruhe, Germany). The powder blend was vigorously mixed, in the right ratio, in an Al_2O_3 ceramic jar for approximately 30 minutes under vacuum. Then, cylindrical pellets were prepared by uniaxially pressing 3 g of the powder mixture at 200 MPa in a steel die. The MW-assisted synthesis was performed in a MW single mode applicator operating at the frequency of 2450 MHz and used in the predominant E-field configuration: TE_{10n} (Transverse Electric mode with 1 semi-period variation of the electric field along the applicator width, 0 variations along the applicator height, and n variations along the applicator length, with n = 2 or 3 in the configuration employed in this work) [28]. The microwave applicator, schematized in Figure 1, consists of a magnetron generator (MKS-Alter, Reggio Emilia, Italy) with an output power level set to 1 kW, a three ports circulator and a three-stubs tuner (MKS-Alter, Reggio Emilia, Italy) based on the WR-340 rectangular waveguide geometry. The three-stubs tuner and an additional shorting plunger allow realizing impedance matching operations, thus modifying the electromagnetic field distribution along the MW cavity. To increase the microwave absorption, thus reducing the heating time, and to limit the temperature gradient generated during the heating, the "two ways hybrid microwave heating" mode was utilized. A crucible made of a MW-susceptor (SiC) was used: thus, the susceptor heats the material from the surface, while the MWs heat it from the core. In this way the material undergoes a more uniform heating compared to the direct microwave heating, where the centre often remains at a higher temperature with respect to the surface [22,29]. A layer of low loss porous alumina was exploited to thermally insulate the crucible without being directly microwave-heated. Furthermore, a porous alumina lid has been placed over the crucible in order to limit heat dissipation and the air exposure of the sample.
Different mixtures of powder and irradiation times were used in order to verify possible Mn losses during the synthesis, due to the experimental setup used. In this work, we report the results for the preparation conditions as optimized in order to synthesize the stoichiometric compound ($Ni_{50}Mn_{25}Sn_{25}$). Particularly, the optimal synthesis resulted from a 50:30:20 mixture of Ni, Mn and Sn powder; the pellet was irradiated with a forward microwave power of 1000 W for 2 minutes. The measurement of the reflected power during the synthesis process showed that most of the incoming power was absorbed by the load (sample and the SiC susceptor). This means that most of the energy was transmitted directly to the material. From the experimental power *vs.* time plot collected during the experiment, a total energy consumption of 120 kJ was calculated, the latter increasing to *ca.* 170 kJ by considering an average magnetron efficiency of 70%. By dividing this value by the mass of the sample treated (i.e. 3 g) the specific energy consumption value of 57 kJ/g is obtained. This value is comparable with the typical energy consumption to arc-melt similar mass of sample. However, considering the long annealing treatments usually performed on arc-melted samples, the gain in terms of energy footprint of the proposed synthesis process is evident. Moreover, it has been demonstrated for different

microwaves driven processes and equipment, that, regardless of the process and equipment employed, by moving from a 5 g scale to a 200 g scale, the specific energy consumption decreases, remaining nearly constant above a 200 g scale, until the full microwave absorption of the emitted power occurs and the surface to volume ratio of the load is decreased [30].

A special experiment was performed to estimate the temperature reached by the material during the synthesis. A sapphire fibre (Mikron M680 Infraducer, Mikron Infrared) was positioned in contact with the sample. The maximum measured temperature during the synthesis was about 1070 K, after *ca.* 100 s of MW irradiation. This means that during the synthesis the sample surface did not reach the melting temperature of the stoichiometric compound (about 1400 K) [15].

The effective composition of the presented sample ($Ni_{50.7\pm0.2}Mn_{25.1\pm0.3}Sn_{24.2\pm0.4}$) was measured by Energy Dispersive X-Ray Spectroscopy (EDS, Inca-350, Oxford Instruments) on a Scanning Electron Microscope (ESEM Quanta 200 Fei, Oxford Instruments). The crystallographic phase was determined through powder X-ray diffraction (XRD) with a PANAlytical X'Pert PRO diffractometer (Cu-Kα radiation, λ = 1.5405 Å). The grinded powder was not annealed after the crushing in order to avoid any possible modification of the crystallographic phase due to the heat treatment [31]. Figure 2 shows the X-ray pattern collected at room temperature for the studied composition. The Le-Bail analysis, performed with the Jana2006 software [32], confirmed the expected cubic $L2_1$ structure (space group Fm-3m) of the austenitic Heusler phase with a cell parameter of 6.030(1) Å. The cell parameter is slightly lower than that reported for $Ni_{50}Mn_{25}Sn_{25}$ compound in [33]. This small difference can be due to the Ni excess, as observed in [34]. A secondary phase was identified as the cubic phase of manganese oxide (MnO). This secondary phase has grown during the synthesis in air of the compound, and it can be avoided by performing the synthesis in a protected atmosphere. However, in the following it is demonstrated that the presence of this minority phase does not degrade the functional properties of the Heusler compound. No traces of Ni_3Sn_2 were observed, differently from [34], most likely due to the faster cooling rate that the sample undergoes compared to that used in [34].

Optical microscopy and backscattered electrons SEM images (one example is shown in the inset of Figure 2), obtained on a polished cross section of the as synthesised specimen, reveal the presence of a porous microstructure with different phases. From the comparison between the measured density (6700±300 kgm^{-3}) and the theoretical full density (about 8800 kgm^{-3}), calculated on the basis of the cell parameter, we estimated a volume porosity of about 24±4%. The porous microstructure is characteristic of powder metallurgy products and, in this case, it is promoted by the gases release during the synthesis due to the Mn sublimation, that starts at 970 K, and to the MnO evaporation [35,36]. This was confirmed by the observation of the rise in Mn loss by increasing the microwave heating (losses of about 5wt% for 2 min of irradiation, 9wt% for 4 min and 10wt% for 6 min). By combining the information obtained from EDS and XRD pattern analysis, 3 phases were identified: the main austenitic Heusler phase (light grey in the SEM image of Figure 2) with grains of several tens of micrometres; the MnO phase, which is found in correspondence of the pores (dark grey), and a phase that surrounds the austenite, which can be identified as a γ-(Ni,Mn) solid solution [15,34]. By increasing the MW irradiation time, we observed a reduction of the porosity (19±4% for 4 minutes irradiation and 16±4% for 6 minutes irradiation, corresponding to a density of 7100±300 kgm^{-3} and 7400±300 kgm^{-3}) and an enlargement of the austenite grains dimension. The observed very rapid grain growth supports the assumption that MW heating enhances the atomic diffusion compared to other heating techniques [37], probably due to localized overheating of the particles surface and electric field concentration in the space existing between particles.

EDS measurements and microscopy observations, performed on different pieces of the prepared samples, confirmed the very good spatial homogeneity of composition and microstructure. This was promoted by the pre-mixing of starting powders and by the reduction of thermal gradients in the sample during the synthesis, through the implementation of the "two ways hybrid microwave heating" method.

Magnetization measurements of the synthesized compound were performed by a Superconductive Quantum Interference Device (SQUID) magnetometer (Quantum Design MPMS-XL5) and a Vibrating Sample Magnetometer (VSM) in the Physical Properties Measurements System (PPMS) DynaCool (Quantum Design). The magnetization as a function of temperature was measured between 5 and 350 K in a small applied magnetic field ($\mu_0 H$ = 0.01 T) to reveal the presence of magnetic phase transitions. Only the ferro to paramagnetic transition of the austenitic phase was observed at 315±1 K. The second-order nature of this transition was confirmed by the Arrott plots (inset of Figure 3), built with the *M(T)* data collected at different applied magnetic fields around the critical temperature (Figure 3). Above the Curie transition the magnetization is approaching zero, demonstrating that the secondary phases (MnO and γ-(Ni,Mn)) give a negligible contribution to the total magnetization of the sample. The saturation magnetization of the austenitic phase, measured at 5 K, is 66±1 Am^2kg^{-1}, comparable with results reported in [38,39]. Instead, the obtained T_c is significantly lower compared to previous results [38–40], probably due to a different degree of atomic order.

The magnetocaloric performance of the compound was measured by direct and indirect methods. The isothermal entropy change (Δs_T) was derived by applying the Maxwell relation at the *M(T)* measurements performed around the transition with different applied magnetic fields in the 0-2 T range (Figure 3) [41]. The $\Delta s_T(T)$ of the sample is reported in the bottom panel of Figure 4 for three different field changes ($\mu_0 \Delta H$ = 1.0, 1.5, 2.0 T). The $\Delta s_T(T)$ reaches a maximum value of 1.4 ± 0.1 $Jkg^{-1}K^{-1}$ for $\mu_0 \Delta H$ = 2 T. The adiabatic temperature change (ΔT_{ad}) was directly measured by an homemade experimental setup based on a Cernox temperature sensor [42]. The temperature variation of the sample induced by a magnetic field change of 1.0, 1.5 and 2.0 T is reported as a function of temperature in the top panel of Figure 4. The direct ΔT_{ad} measurements were performed on a parallelepiped sample (a = 4.6 mm, b = 3.2 mm, c = 1.6 mm) with the magnetic field applied along the b axis. By considering the ellipsoidal approximation, a demagnetizing field of about 0.04 T at the maximum ΔT_{ad} is estimated. The maximum ΔT_{ad} is 0.8 ± 0.1 K for a field change of 2 T. The MCE is completely reversible, as expected in the case of second order magnetic transitions. The MC parameters result in agreement with previously published data, considering, for the comparison of the presented results with other NiMnSn compositions, the linear behaviour of both Δs_T and ΔT_{ad} with the saturation magnetization [18,43–45].

In conclusion, it has been shown that $Ni_{50}Mn_{25}Sn_{25}$ Heusler compound can be efficiently and quickly synthesized starting from elemental compacted powders by using microwave heating in hybrid mode. This method involves the use of a composite crucible formed by SiC susceptors and an external insulating lining in porous alumina. The prepared sample shows very good structural, magnetic and magnetocaloric properties, comparable with those reported in literature for materials synthetized by arc-melting and subsequent long annealing treatments at high temperature. The here proposed one-step procedure represents an extremely fast method to produce multifunctional Heusler compounds, with a gain in terms of energy efficiency, economically feasibility and environmental impact. Moreover, the large adaptability and the possibility to merge the synthesis and sintering processes to cast customized shapes, make the presented method a possible solution to develop scale-up routes for a mass production of Heusler compounds for technological applications.

Acknowledgements

FC and NSA gratefully acknowledge funding by the Regione Emilia-Romagna via the 2014-20 POR-FESR program ("FriMag" Project, CUP E32F16000190007). SC would like to thank Gavin Stenning for help on the PPMS instrument in the Materials Characterisation Laboratory at the ISIS Neutron and Muon Source.

References

[1] T. Graf, C. Felser, S.S.P. Parkin, Prog. Solid State Chem. 39 (2011) 1–50.
[2] R.A. Kishore, S. Priya, Renew. Sustain. Energy Rev. 81 (2018) 33–44.
[3] A. Kitanovski, J. Tušek, U. Tomc, U. Plaznik, M. Ožbolt, A. Poredoš, Magnetocaloric Energy Conversion From Theory to Applications, Springer I, 2015.
[4] J. Liu, T. Gottschall, K.P. Skokov, J.D. Moore, O. Gutfleisch, Nat. Mater. 11 (2012) 620–626.
[5] S. Singh, L. Caron, S.W. D'Souza, T. Fichtner, G. Porcari, S. Fabbrici, C. Shekhar, S. Chadov, M. Solzi, C. Felser, Adv. Mater. 28 (2016) 3321–3325.
[6] S. Fabbrici, G. Porcari, F. Cugini, M. Solzi, J. Kamarad, Z. Arnold, R. Cabassi, F. Albertini, Entropy 16 (2014) 2204–2222.
[7] T. Krenke, M. Acet, E.F. Wassermann, X. Moya, L. Mañosa, A. Planes, Phys. Rev. B - Condens. Matter Mater. Phys. 73 (2006) 174413.
[8] G. Cavazzini, F. Cugini, M.E. Gruner, C. Bennati, L. Righi, S. Fabbrici, F. Albertini, M. Solzi, Scr. Mater. 170 (2019) 48–51.
[9] G. Porcari, K. Morrison, F. Cugini, J.A. Turcaud, F. Guillou, A. Berenov, N.H. Van Dijk, E.H. Brück, L.F. Cohen, M. Solzi, Int. J. Refrig. 59 (2015) 29–36.
[10] V. Recarte, J.I. Pérez-Landazábal, V. Sánchez-Alarcos, J.A. Rodríguez-Velamazán, Acta Mater. 60 (2012) 1937–1945.
[11] V.D. Buchelnikov, P. Entel, S. V. Taskaev, V. V. Sokolovskiy, A. Hucht, M. Ogura, H. Akai, M.E. Gruner, S.K. Nayak, Phys. Rev. B - Condens. Matter Mater. Phys. 78 (2008) 184427.
[12] F. Cugini, G. Porcari, S. Fabbrici, F. Albertini, M. Solzi, Philos. Trans. R. Soc. A Math. Phys. Eng. Sci. 374 (2016) 20150306.
[13] F. Cugini, G. Porcari, T. Rimoldi, D. Orsi, S. Fabbrici, F. Albertini, M. Solzi, JOM 69 (2017) 1422–1426.
[14] F. Cugini, L. Righi, L. Van Eijck, E. Brück, M. Solzi, J. Alloys Compd. 749 (2018) 211–216.
[15] M. Yin, J. Hasier, P. Nash, J. Mater. Sci. 51 (2016) 50–70.
[16] R.A. Ahamed, R. Ghomashchi, Z. Xie, L. Chen, Materials 11 (2018) 988.
[17] H. Zhang, M. Qian, X. Zhang, S. Jiang, L. Wei, D. Xing, J. Sun, L. Geng, Mater. Des. 114 (2017) 1–9.
[18] F. Cugini, D. Orsi, E. Brück, M. Solzi, Appl. Phys. Lett. 113 (2018) 232405.
[19] C.S. Birkel, W.G. Zeier, J.E. Douglas, B.R. Lettiere, C.E. Mills, G. Seward, A. Birkel, M.L. Snedaker, Y. Zhang, G.J. Snyder, T.M. Pollock, R. Seshadri, G.D. Stucky, Chem. Mater. 24 (2012) 2558–2565.
[20] C.S. Birkel, J.E. Douglas, B.R. Lettiere, G. Seward, N. Verma, Y. Zhang, T.M. Pollock, (2013) 6990–6997.
[21] Y. Lei, Y. Li, L. Xu, J. Yang, R. Wan, 660 (2016) 166–170.
[22] M. Gupta, E.W.W. Leong, Microwaves and Metals., John Wiley & Sons, 2007.
[23] R. Rosa, P. Veronesi, C. Leonelli, Chem. Eng. Process. 71 (2013) 2–18.
[24] P.K. Loharkar, A. Ingle, S. Jhavar, J. Mater. Res. Technol. 8 (2019) 3306–3326.
[25] R. Rosa, L. Trombi, P. Veronesi, C. Leonelli, Int. J. Self-Propagating High-Temperature Synth. 26 (2017) 221–233.

[26] G. Poli, R. Sola, P. Veronesi, Mater. Sci. Eng. A 441 (2006) 149–156.
[27] S. Raynova, M.A. Imam, F. Yang, L. Bolzoni, J. Manuf. Process. 39 (2019) 52–57.
[28] R. Rosa, L. Trombi, A. Casagrande, F. Cugini, C. Leonelli, P. Veronesi, Mater. Chem. Phys. 233 (2019) 220–229.
[29] M. Bhattacharya, T. Basak, Energy 97 (2016) 306–338.
[30] J.M. Bermúdez, D. Beneroso, N. Rey-Raap, A. Arenillas, J.A. Menéndez, Chem. Eng. Process. 95 (2015) 1–8.
[31] A. Çakır, M. Acet, J. Magn. Magn. Mater. 448 (2018) 13–18.
[32] V. Petříček, M. Dušek, L. Palatinus, Zeitschrift Für Krist. - Cryst. Mater. 229 (2014) 345–352.
[33] S. Aksoy, T. Krenke, M. Acet, E.F. Wassermann, X. Moya, L. Mañosa, A. Planes, Appl. Phys. Lett. 91 (2007) 2005–2008.
[34] M. Yin, P. Nash, W. Chen, S. Chen, J. Alloys Compd. 660 (2016) 258–265.
[35] E. Hryha, E. Dudrov, in:, Appl. Thermodyn. to Biol. Mater. Sci., Ed. InTech, 2011.
[36] A. Šalak, M. Selecká, Manganese in Powder Metallurgy Steels, Cambridge International Science Publishing Ltd., Cambridge, 2012.
[37] J.D. Katz, Annu. Rev. Mater. Sci. 22 (1992) 153–170.
[38] T. Krenke, M. Acet, E.F. Wassermann, X. Moya, L. Mañosa, A. Planes, Phys. Rev. B - Condens. Matter Mater. Phys. 72 (2005) 014412.
[39] A. Çakir, L. Righi, F. Albertini, M. Acet, M. Farle, Acta Mater. 99 (2015) 140–149.
[40] J. Kübler, G.H. Fecher, C. Felser, Spintron. From Mater. to Devices 28 (2013) 71–95.
[41] G. Porcari, F. Cugini, S. Fabbrici, C. Pernechele, F. Albertini, M. Buzzi, M. Mangia, M. Solzi, Phys. Rev. B - Condens. Matter Mater. Phys. 86 (2012) 104432.
[42] G. Porcari, M. Buzzi, F. Cugini, R. Pellicelli, C. Pernechele, L. Caron, E. Brück, M. Solzi, Rev. Sci. Instrum. 84 (2013) 073907.
[43] N.H. Dan, N.H. Duc, N.H. Yen, P.T. Thanh, L. V. Bau, N.M. An, D.T.K. Anh, N.A. Bang, N.T. Mai, P.K. Anh, T.D. Thanh, T.L. Phan, S.C. Yu, J. Magn. Magn. Mater. 374 (2015) 372–375.
[44] V. V. Khovaylo, K.P. Skokov, O. Gutfleisch, H. Miki, T. Takagi, T. Kanomata, V. V. Koledov, V.G. Shavrov, G. Wang, E. Palacios, J. Bartolomé, R. Burriel, Phys. Rev. B 81 (2010) 214406.
[45] K. Dadda, S. Alleg, S. Souilah, J.J. Suñol, E. Dhahri, L. Bessais, E.K. Hlil, J. Alloys Compd. 735 (2018) 1662–1672.

Figures

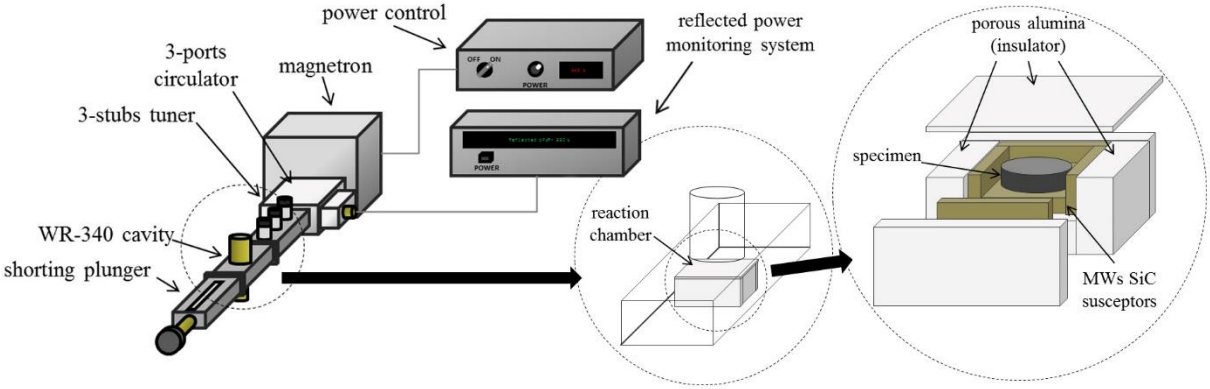

Figure 1. Detailed scheme of the microwave single mode applicator used for the synthesis performed in the predominant E-field configuration with MW SiC susceptor.

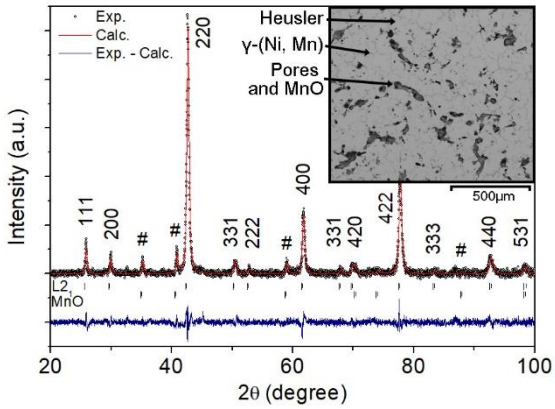

Figure 2 X-ray powder diffraction pattern of the $Ni_{50}Mn_{25}Sn_{25}$ sample collected at room temperature. The indexed peaks correspond to the $L2_1$ Heusler phase. The # peaks fit the MnO phase. Inset: Backscattered SEM image of the sample surface.

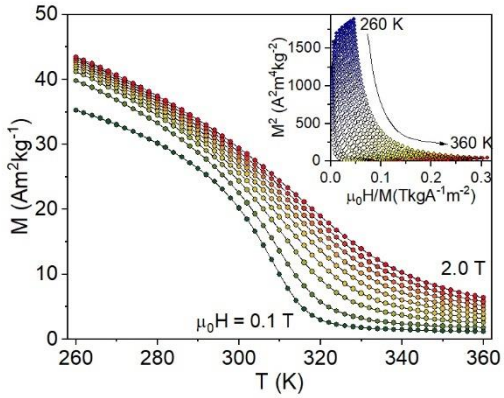

Figure 3 Magnetizatio of $Ni_{50}Mn_{25}Sn_{25}$ as a function of temperature at different applied magnetic fields ($\mu_0 H$ from 0.1 T to 2.0 T). Inset: Arrott plots of the M(T) data.

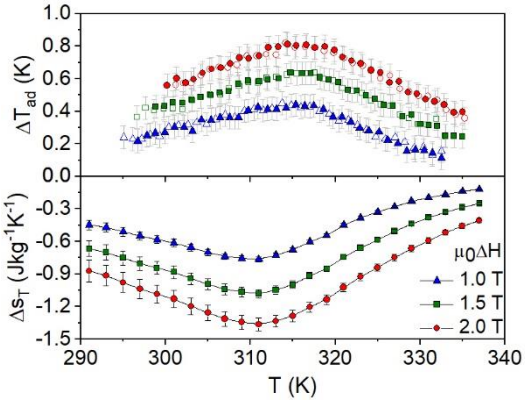

Figure 4 Top panel: adiabatic temperature change directly measured on heating (filled symbols) and on cooling (empty symbols) with an applied magnetic field of 1.0 T (triangles), 1.5 T (squares) and 2.0 T (circles). Bottom panel: isothermal entropy change derived from magnetization data for a magnetic field variation of 1.0 T (triangles), 1.5 T (squares) and 2.0 T (circles).